





Inhibition of *Leishmania infantum* trypanothione reductase by diaryl sulfide derivatives

Francesco Saccoliti^{a*}, Gabriella Angiulli^{b*}, Giovanni Pupo^a, Luca Pescatori^a, Valentina Noemi Madia^a, Antonella Messori^a, Gianni Colotti^b, Annarita Fiorillo^b, Luigi Scipione^a , Marina Gramiccia^c, Trentina Di Muccio^c, Roberto Di Santo^a , Roberta Costi^{a*†}  and Andrea Ilari^{b*†} 

^aIstituto Pasteur-Fondazione Cenci Bolognetti, Dipartimento di Chimica e Tecnologie del Farmaco, “Sapienza” Università di Roma, Roma, Italia;

^bIstituto di Biologia e Patologia Molecolari – CNR, and Dipartimento di Scienze Biochimiche, “Sapienza” Università di Roma, Roma, Italia;

^cDipartimento di Malattie Infettive, Parassitarie e Immunomediate, Istituto Superiore di Sanità, Roma, Italia

ABSTRACT

The study presented here aimed at identifying a new class of compounds acting against *Leishmania* parasites, the causative agent of Leishmaniasis. For this purpose, the thioether derivatives of our in-house library have been evaluated in whole-cell screening assays in order to determine their *in vitro* activity against *Leishmania* protozoan. Among them, promising results have been achieved with compound RDS 777 (6-(sec-butoxy)-2-((3-chlorophenyl)thio)pyrimidin-4-amine) (IC₅₀ = 29.43 μM), which is able to impair the mechanism of the parasite defence against the reactive oxygen species by inhibiting the trypanothione reductase (TR) with high efficiency (K_i 0.25 ± 0.18 μM). The X-ray structure of *L. infantum* TR in complex with RDS 777 disclosed the mechanism of action of this compound that binds to the catalytic site and engages in hydrogen bonds the residues more involved in the catalysis, namely Glu466', Cys57 and Cys52, thereby inhibiting the trypanothione binding and avoiding its reduction.

ARTICLE HISTORY

Received 3 August 2016

Revised 26 September 2016

Accepted 28 September 2016





KEYWORDS

Diaryl sulfide derivatives; *Leishmania infantum*; trypanothione reductase; trypanothione reductase inhibition; X-ray crystal structure

Introduction

The parasitic protozoan *Leishmania*, is the causative agent of Leishmaniasis, a neglected tropical disease throughout the world. Human Leishmaniasis consists of the following three major clinical forms: visceral Leishmaniasis (VL), which is fatal if left untreated, cutaneous Leishmaniasis, which can heal spontaneously but leaves disfiguring scars, and mucocutaneous Leishmaniasis, which is not self-healing and can be potentially fatal. VL causes an estimated 60 000 deaths annually (a rate surpassed among parasitic diseases only by malaria)^{1,2}. *Leishmania*, together with other protozoan pathogens, that is, all species of *Trypanosoma*, belongs to the Trypanosomatidae family. The therapy of such infections represents a neglected area of research and drug development. Nowadays, treatment of these diseases is unsatisfactory in terms of safety and efficacy, which sharply contrasts with the therapeutic need in terms of people at risk, number of affected patients and associated fatalities. This discrepancy is primarily due to the distribution of these infections in tropical and subtropical poor countries that do not represent an attractive market for pharmaceutical companies and have limited research capacities and public health infrastructure. As a consequence, efficacious new drugs have not been developed yet, and the available ones still comprise the highly toxic antimony-containing compounds (i.e. glucantime and pentostam). For this reason, there is an urgent need to find new and more affordable drug-targeting protein essential for the parasite survival but absent in the human host. Instead of the

mammalian redox defence machinery based on glutathione, the trypanosomatid parasites possess trypanothione as the main defending system against oxidative damage. Trypanothione, [N1,N8-bis(glutathionyl)spermidine] (TS₂), which is synthesized by trypanothione synthetase (TryS) and reduced to T(SH)₂ by the trypanothione reductase (TR), is used by the couple tryparedoxin/tryparedoxin peroxidase I (TXN/TXNpx) to neutralize the hydrogen peroxide produced by the macrophages during the infection^{3,4}. All attempts to obtain a TR-null mutant in *Leishmania (L.) donovani* failed and mutants, displaying a partial trisomy of TR locus, where two TR alleles were disrupted by gene targeting, show attenuated infectivity and decreased ability to survive within the macrophages⁵. Thus, due to the essential role played by TR in trypanosomatids and its absence in the human host, trypanothione reductase represents an attractive target for the development of new potential drugs. The crystal structure of *L. infantum* TR has recently been solved⁶ and has been shown to be very similar to the structure of other trypanosomatid TR solved so far, that is, TR from *Chitidia (C.) fasciculata* and from *T. cruzi*. TR is a homodimer in which each subunit is formed by three domains: the interface domain (361–488), the NADPH-binding domain (residues 161–289) and the FAD-binding domain (residues 1–160 and 289–360). The trypanothione-binding site is placed in a big cavity at the interface between the two domains formed by the residues of the FAD-binding site of one domain and the residues of the interface domain of the twofold symmetry related subunit. The trypanothione is reduced by NADPH in a TR-catalyzed reaction with the

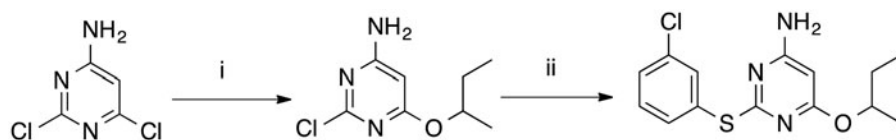
CONTACT Roberta Costi  roberta.costi@uniroma1.it  Istituto Pasteur-Fondazione Cenci Bolognetti, Dipartimento di Chimica e Tecnologie del Farmaco, “Sapienza” Università di Roma, Roma, Italia; Andrea Ilari  andrea.ilari@uniroma1.it  Istituto di Biologia e Patologia Molecolari – CNR, Roma, Italia

*These authors contributed equally to this work.

†Cosenior authorship.

© 2017 The Author(s). Published by Informa UK Limited, trading as Taylor & Francis Group

This is an Open Access article distributed under the terms of the Creative Commons Attribution License (<http://creativecommons.org/licenses/by/4.0/>), which permits unrestricted use, distribution, and reproduction in any medium, provided the original work is properly cited.



Scheme 1. Synthesis of RDS 777. (i) *sec*-BuOH, Na, reflux, 4 h, 50%^{12,13}; (ii) 3-chlorothiophenol, Pd₂(dba)₃, DPPF, DIPEA, DMF, reflux, 6.5 h, 68.33%.

following mechanism: the two NADPH electrons are transferred via FAD to the Cys52-Cys57 disulfide bridge. When TS₂ binds to the protein, Cys52, deprotonated by the couple His461'-Glu466', attacks nucleophilically the trypanothione disulfide bridge with the formation of a mixed disulfide bridge and finally, the attack of the second protein cysteine (Cys57) on Cys52 produces the reduced substrate. Baiocco et al. have shown that one of the mechanisms of action of the antimonial drugs is the inhibition of TR activity⁶. Sb(III) is able to inhibit TR (K_i = 1.5 μM), thereby killing the *Leishmania* parasites. The structure of the Sb(III)-TR complex shows that Sb(III) inhibits TR catalytic activity by binding to the residues involved in catalysis, namely Cys52, Cys57 and His461'. Several metals, such as Terpyridine platinum (II) complexes, gold (I) derivatives and silver polypyridyl complexes, can be effective against *Leishmania* spp.⁶. The X-ray structures of the Ag(I)- and Au(I)-TR from *L. infantum* disclosed that all the metals that are Lewis soft acids can bind to the two TR catalytic cysteines, thereby inhibiting TR activity with a mechanism similar to that described for Sb(III)^{7,8}. Several organic compounds, such as acridines, 2- and 3-substituted 1,4-naphthoquinone derivatives, peptides and aniline-based diarylsulfides, were designed on the basis of TR crystal structure, as specific TR inhibitors⁹. Spinks et al. tested 62 000 compounds on *T. brucei* TR using a high-throughput screening method based on the classical TR enzymatic assay coupled to the DTNB (5,5'-dithiobis-(2-nitrobenzoic acid)) reduction followed at 405 nm. They identified two series of compounds, based on quinoline and pyrimidopyridazine scaffolds, showing good selectivity over the human homolog glutathione reductase (GR) and able to inhibit TR in the micromolar range^{10,11}.

In spite of various efforts to discover potent TR inhibitors that did not block the closest mammalian homolog, glutathione reductase (GR), only a small number of compounds have been found to have good anti-parasitic activity. An explanation was given by the studies on conditioned TR knockout in *T. brucei* where it was demonstrated that only the parasites with a TR wild-type activity lower than 10% are unable to grow and infect mice⁵. For this reason, TR should be inhibited at submicromolar range to prevent parasite growth due to the endogenous substrate accumulation, which may displace a competitive inhibitor with low affinity. In this framework, our studies aimed at identifying a new class of compounds acting against *Leishmania* parasites in submicromolar range. We evaluated our in-house library of compounds previously synthesized and endowed with different biological activities. In particular, our in-house diaryl sulfide derivatives, previously synthesized as anti-HIV agents^{12,13}, have been evaluated in whole-cell screening assays for determining their *in vitro* activity against *Leishmania* parasites. Among them, promising results have been achieved with compound RDS 777, which is able to inhibit the promastigotes growth by binding with high affinity to the catalytic site of TR.

Materials and methods

Chemistry

Compound RDS 777 was synthesized as previously described in the literature¹³; however, we decided to modify the second reaction

step applying a modified Buchwald-Hartwig C-S cross coupling reaction¹⁴, as depicted in **Scheme 1**, in order to avoid the use of thiophenol potassium salt (difficult to handle) and reduce the reaction time required, in spite of its reduced yield. Melting point (°C), recrystallization solvent, yield (%), chromatographic system, IR, ¹H-NMR, formula, Mr and analyzed elements for derivatives RDS 738 and RDS 777 are described in literature^{12,13}. All compound samples used for biological evaluation were determined to be 99% pure as determined by elemental analysis.

6-(*Sec*-butoxy)-2-((3-chlorophenyl)thio)pyrimidin-4-amine (RDS 777)

Compound RDS 738 (1 g; 4.96 mmol) was added to a well-stirred solution of Pd₂(dba)₃ (45.42 mg; 49.6 μmol), DPPF (55.28 mg; 99.18 μmol), DIPEA (0.95 ml; 5.45 mmol) and 3-chlorobenzenthio (0.576 ml; 4.96 mmol) in anhydrous DMF (7.5 ml) at room temperature. The solution was stirred under reflux for 6.5 h; the mixture was cooled to room temperature, treated with water (50 ml) and extracted with chloroform (3 × 50 ml). The collected extracts were washed with brine (3 × 100 ml) and dried. Removal of the solvent furnished crude residue that was purified by CC (SiO₂; *n*-hexane: acetone 5:1), yielding RDS 777 (1.05 g, 68.33%) as a white-yellow solid.

In vitro experiments: inhibition of promastigote growth

Promastigote (the extracellular stage of the *Leishmania* life cycle) growth inhibition was evaluated using *L. infantum* strain (MHOM/TN/80/IPT1). To estimate the 50% inhibitory concentration (IC₅₀), the MTT (3-[4,5-dimethylthiazol-2-yl]-2,5-diphenyltetrazolium bromide) micromethod¹⁵ was used throughout the experiments with modification. Promastigotes were grown in Schneider's *Drosophila* medium (SIGMA) containing 10% fetal calf serum (FCS) (GIBCO-BRL) and 2% gentamicin (50 mg/l) (Sigma) at 22 °C. Parasites were adjusted to 1 × 10⁶ parasites/ml, and 200 μl of suspension was seeded in triplicate in 96-well flat-bottom microplates and incubated with varying concentrations of RDS 777 compound from stock solution in DMSO: 256, 128, 64, 32, 16, 8, 4, 2, 1, 0.5, 0.25, 0.125, 0.062, 0.031 μM. Amphotericin B (Euroclone) (AmB) was used as control at various concentrations: 8, 4, 2, 1, 0.5, 0.25, 0.125, 0.062 μM. A DMSO control was assayed in parallel with the concentration of DMSO never exceeding 1%. Each experiment was done in triplicate for each drug concentration and two independent experiments were performed. After 72 h of incubation, 30 μl of MTT was added to each well and plates were further incubated for 2 h. The absorbance at 550 nm was measured with a 96-well scanner. Antileishmanial activity was expressed as a percentage of the reduction in the number of live parasites compared to the control (non-treated parasites). In addition, the promastigote vitality was followed by microscopic observation after 72 h. Results were analyzed by GraphPad Prism 3 (San Diego, CA).

Enzymatic assay

L. infantum TR was cloned and purified as previously described^{6,16}. Enzyme inhibition assays were carried out at 25 °C using a diode array Hewlett-Packard HP8452A spectrophotometer. The solution

containing TR 40 nM, TS₂ (75 μM, 100 μM, 200 μM, 400 μM) and RDS777 (50 nM, 100 nM, 250 nM, 500 nM, 1 μM, 5 μM, 10 μM) were allowed to equilibrate for 2 min in a quartz cuvette. Assays were initiated by the addition of NADPH 40 μM and the absorbance decrease at 340 nm, which indicates the oxidation of NADPH, was followed. The concentrations of NADPH was calculated using the molar extinction coefficient $\epsilon=6222 \text{ /M/cm}$ at 340 nm. Trypanothione disulfide (Bachem) and NADPH (Sigma) were used for the experiments.

X-ray structure determination

Crystallization of TR from *L. infantum* were carried out as previously reported^{6,16}. The crystals grew at a controlled temperature of 294 K, reaching dimension of 0.3 mm × 0.3 mm × 0.2 mm in about 7 days. Crystals of the native oxidized TR were soaked for 1 h using a stabilizing solution containing 1.5 M ammonium sulfate, 0.1 M Tris pH 8.5 and 2 mM inhibitor. Crystals were cryo-protected in a solution containing 2.0 M sodium malonate. Then, the crystals were flash-frozen by quick submersion into liquid nitrogen for transport to a synchrotron radiation source.

Single wavelength data sets ($\lambda=0.918 \text{ \AA}$) were collected at the beamline BL 14-1 at the Synchrotron Radiation Source BESSY¹⁷, Berlin, Germany, using a CCD detector at a temperature of 100 K. The data sets were processed and scaled with XDS¹⁸. The crystals belong to the P41 space group with the following cell dimensions: $a=102.5 \text{ \AA}$, $b=102.5 \text{ \AA}$, $c=192 \text{ \AA}$. Crystal parameters and complete data collection statistics are reported in Table 1. The structures of *L. infantum* TR in complex with RDS777 were solved by molecular replacement using as search model the native TR (pdb code 2JK6)⁶ with the program Molrep¹⁹. Refinement was performed using the program REFMAC5²⁰ and model building was carried out using the program COOT²¹. The structure of TR in complex with RDS777 was refined to a final free *R* value of 23.3% for all resolution shells (50–3.5 Å), calculated using the working set reflections (23 650) and Free *R* value, calculated using the test set reflections (1621), of 35.6%. The final model is a dimer containing

Table 1. Crystal parameters, data collection statistics and refinement statistics of RDS777–TR complex

Space group	P41
Unit cell parameters	
<i>a</i> (Å)	102.5
<i>b</i> (Å)	102.5
<i>c</i> (Å)	192
Number of molecule in the asymmetric unit	2
Wilson plot B factor (Å ²)	95.5
Data statistics	
Resolution range	3.5–48 (3.5–3.7)
Unique reflections	24 914 (3949)
Completeness	99.6 (98.1)
Redundancy	5.12 (5.04)
<i>R</i> _{merge} (%)*	23 (117)
CC1/2	99 (75.1)
<i>I</i> / σ (<i>I</i>)	8.2 (1.7)
Structure refinement	
Resolution range	3.5–48 (3.5–3.6)
Reflection in bins	23 650 (1666)
<i>R</i> _{crys} (%)	21 (36)
<i>R</i> _{free} (%)	23 (36)
Rms bonds (Å)	0.009
Rms angle (°)	1.4
Ramachandran plot	
Residues in core region (%)	92
Residues in allowed region (%)	8

Values in parentheses are for the high-resolution shell.

* $R_{\text{merge}} = \frac{\sum hkl \sum i |I_i(hkl) - I(hkl)|}{\sum hkl \sum_i I_i(hkl)}$, where $I_i(hkl)$ is the *i*th observation of the reflection (*hkl*) and $I(hkl)$ is the mean intensity of the (*hkl*) reflection.

974 residues (486 for monomer A and 487 for monomer B), two FAD molecules, one sulfate molecule and seven RDS777 molecules (three in the monomer A and four in the monomer B). The most favored regions of the Ramachandran plot contains 92.0% of residues, the allowed regions contain the 8.0% of residues. The X-ray structure has been deposited in the protein data bank with the PDB code 5EBK.

Results and discussion

Activity against Leishmania promastigotes assays

Stump et al. already have shown that some diaryl sulfides are able to inhibit *T. brucei* TR, thereby killing the protozoan (some of them displayed an IC₅₀ in the micromolar range)²².

On this basis, we evaluated our in-house library of diaryl sulfide compounds previously synthesized and endowed with different biological activities against *Leishmania infantum* promastigotes. In particular, our in-house diaryl sulfide derivatives, previously synthesized as anti-HIV agents^{12,13}, have been evaluated in whole cell screening assays for determining their *in vitro* activity against *Leishmania* parasites. Among them, only RDS 777 shows a significant activity against promastigotes.

RDS 777 induced a dose-dependent antiproliferative effect on *L. infantum* promastigotes. Seventy-two hours after treatment, 256–128 μM concentrations of RDS 777 induced 100% promastigote mortality, whereas lower drug concentrations induced a dose-dependent anti-proliferative effect on *L. infantum* promastigotes. IC₅₀ deduced from the dose-response curve was $29.43 \pm 1.34 \mu\text{M}$ (95% CI: 15.94–54.34), (the deduced IC₅₀ of AmB was $0.52 \pm 1.59 \mu\text{M}$; 95% CI: 0.18–1.45) (Figure 1). No effect on promastigotes growth was observed by the presence of up to 1% DMSO in the culture medium. The calculated IC₅₀ is of the same order of magnitude of that calculated for compound 1 (4-((1-(4-ethylphenyl)-2-methyl-5-(4-(methylthio)phenyl)-1H-pyrrol-3-yl)methyl)thiomorpholine), an azole-based compound that has been shown to be able to bind to the trypanothione-binding cavity, against *Leishmania donovani* (13.77 μM)²³.

Enzymatic assay

Steady-state kinetic experiments were carried out at various concentration of TS₂ and inhibitor and at a fixed NADPH

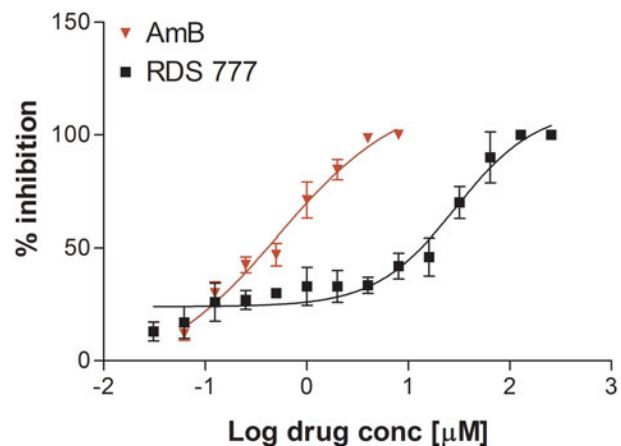


Figure 1. % Inhibition calculated on *L. infantum* promastigote stage after treatment with various concentrations of RDS777 and reference drug Amphotericin B (AmB). The data are expressed as mean ± standard error of two independent experiments.

concentration (40 μM). After starting the reaction by the addition of NADPH, the absorbance decrease at 340 nm, indicating the oxidation of NADPH, was measured. As shown from Figure 2, RDS 777 inhibits competitively the binding of trypanothione to TR. Each line in the Dixon plot (Figure 2) represents linear regression analysis of reciprocal of average simulated rates of trypanothione reduction for different substrate concentrations as a function of inhibitor concentration. The K_M and k_{cat} of TR used for the K_i calculation are $23 \pm 1 \mu\text{M}$ and $11.4 \pm 0.3/\text{s}$ respectively²³. The value of K_i calculated from the Dixon plot analysis is $0.25 \pm 0.18 \mu\text{M}$ six times lower than that of Sb(III) (1.5 μM) the active form of antimonials the most used drug against Leishmaniasis calculated by Baiocco et al⁶ and more than 18 times lower than is that of compound 1 ($4.6 \pm 2.5 \mu\text{M}$)²³.

The RDS 777 K_i value ($0.25 \pm 0.18 \mu\text{M}$) is two order of magnitude lower than the IC_{50} deduced from the dose-response curve ($29.43 \pm 1.34 \mu\text{M}$). Numerous specific and efficient tripanosomatids TR inhibitors have been found to have modest effect on the

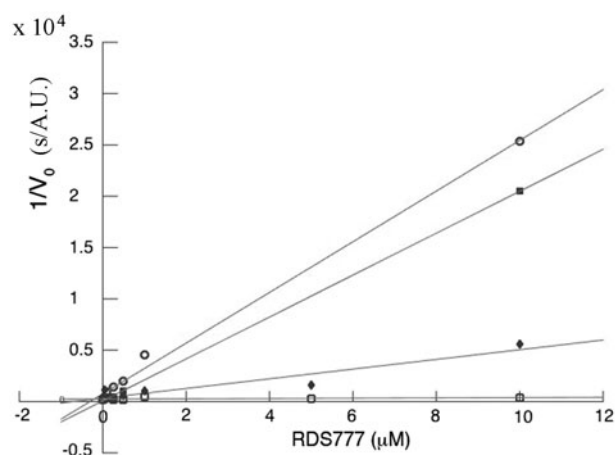


Figure 2. Dixon plot of TR inhibition by RDS777: open circles $[\text{TS}_2] = 75 \mu\text{M}$; filled squares $[\text{TS}_2] = 100 \mu\text{M}$; filled diamonds $[\text{TS}_2] = 200 \mu\text{M}$ and open squares $[\text{TS}_2] = 400 \mu\text{M}$.

parasites grown. A partial explanation was provided by Krieger et al. who produced conditioned TR knockout in *T. brucei*²⁴. They have shown that the redox metabolism of the parasite was affected only when TR was titrated down to less than 5% of normal.

X-ray crystal structure of TR in complex with RDS 777

Stump et al.²² have already shown the ability of diarylsulfide derivatives to bind *T. cruzi* TR and tentatively proposed a modelling-based binding mode for this class of compounds.

In order to study the mechanism of inhibition exerted by this compound and determine the binding mode of the diaryldisulfide derivatives, we solved the X-ray structure of *L. infantum* TR in its oxidized state in complex with RDS 777 (LiTR-777) at 3.5 Å resolution (Figure 3). Apart from few cases, such as previously reported azole-based compounds²³, no binding mode of any competitive *Leishmania* TR inhibitor has been deciphered by protein crystallography to date; thus, the development of novel TR inhibitors has been based on molecular dynamics simulations without X-ray study confirmation. In this sense, our crystallographic study gave us a clear and specific insight of RDS 777-binding mode, highlighting that our compound is involved in some peculiar, well-defined interactions into TR catalytic site.

The X-ray structure of LiTR-777 is identical to the TR-oxidized apo-form. The functional dimer is made of two identical subunits related by a twofold axis (the superimposition between the two monomers A and B yields a rmsd of 0.18 Å). Each monomer contains a FAD molecule. The monomer A binds three RDS 777 molecules, whereas the monomer B binds four RDS 777 molecules. RDS 777 b and c are bound in both monomers to the NADPH-binding site, whereas the RDS 777 a in the monomer A and a and d in monomer B are bound to the trypanothione-binding site (Figure 3). The RDS 777 in position a are bound in similar way in the two monomers (Figure 4(A) and (B)).

Due to the presence of several nonpolar aminoacids within the catalytic site, RDS 777 in position a interacts with the hydrophobic Val53 and Val58 and, furthermore, it is hydrogen bound to the

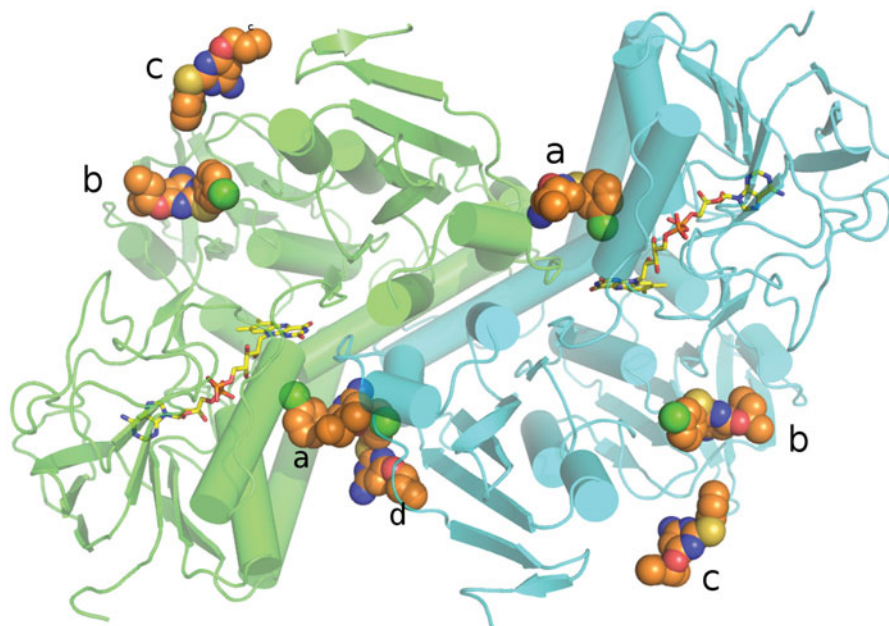


Figure 3. Overall fold of TR in complex with RDS 777. RDS777 is represented as CPK and colored orange and the FAD molecules is represented as sticks and colored in yellow. The seven RDS777 molecules bound to the TR protein are indicated with the a-d letters.

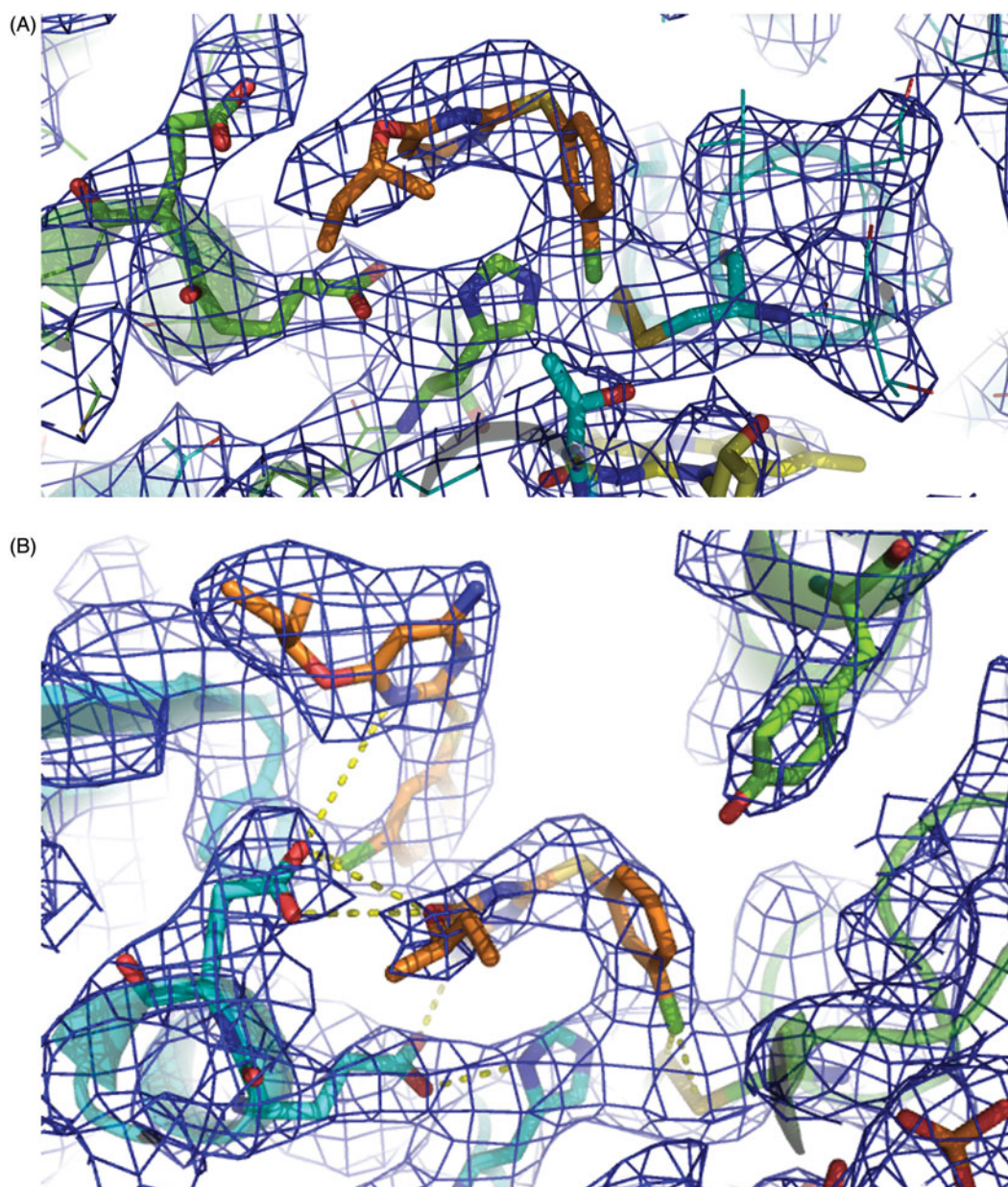


Figure 4. Electronic density map of the RDS777-TR complex active site. (A) 2Fo-Fc map of the monomer A. (B) 2Fo-Fc map of the monomer B. RDS 777 and the residues interacting with the compounds are represented as sticks. The 2Fo-Fc map is colored blue and contoured at 1σ .

residues more involved in the catalysis, namely His 461', Glu466', Cys57, Cys52 and Glu467' (Figure 5(A) and 5(B)). In particular, RDS 777 in position *a* interacts, through the aniline moiety, with the acidic residue Glu466', while the arylsulfide moiety localizes near the hydrophobic Val53 and Val58 and close to Tyr110 a residue important for the trypanothione correct positioning in the cavity²³. Moreover, as shown in the Figure 5(A), the chloride atom of the benzyl chloride moiety forms electrostatic interactions with the sulfur atoms of the two catalytic cysteines (Cys 52 and Cys 57) forming a disulfide bridge. This binding mode is peculiar of our diarylsulfide inhibitor, which, however, enlightens an alternative interaction mode different from the other simulated ones previously described in literature. In particular, the diarylsulfide derivative (3-({5-Chloro-2-[(4'-methylbiphenyl-4-yl)thio]phenyl}amino)-N-(3,4-dichlorobenzyl)-N,N-dimethylpropan-1-ammonium chloride) modeled by Stump et al. in the trypanothione-binding site accommodates in the cavity in a completely different manner. In their model, the diarylsulfide moiety is positioned close to the so-

called "mepacrine"-binding site distant from the two catalytic cysteines.

In the monomer B of LiTR-777 X-ray structure, an additional molecule of RDS 777 binds to the trypanothione-binding site (molecule *d*). This additional molecule displays an occupancy lower than 1 (0.8) and is placed close to the entrance of the trypanothione-binding site. The chloro benzyl moiety of the molecule *d* forms a stacking interaction with the aniline moiety of the molecule *a* and a hydrogen bond with the Glu467'. As shown in Figure 5(C), the binding mode of the diaryl sulfides differs from that of the more bulky diphenyl pyrroles that are placed nearer the entrance of the cavity and farther from the LiTR catalytic triad.

Conclusions

In order to identify novel anti-Leishmanian agents engaged with good activity, we evaluated the antiprotozoan activity of our in-house library of compounds. Among them, RDS 777 proved to be

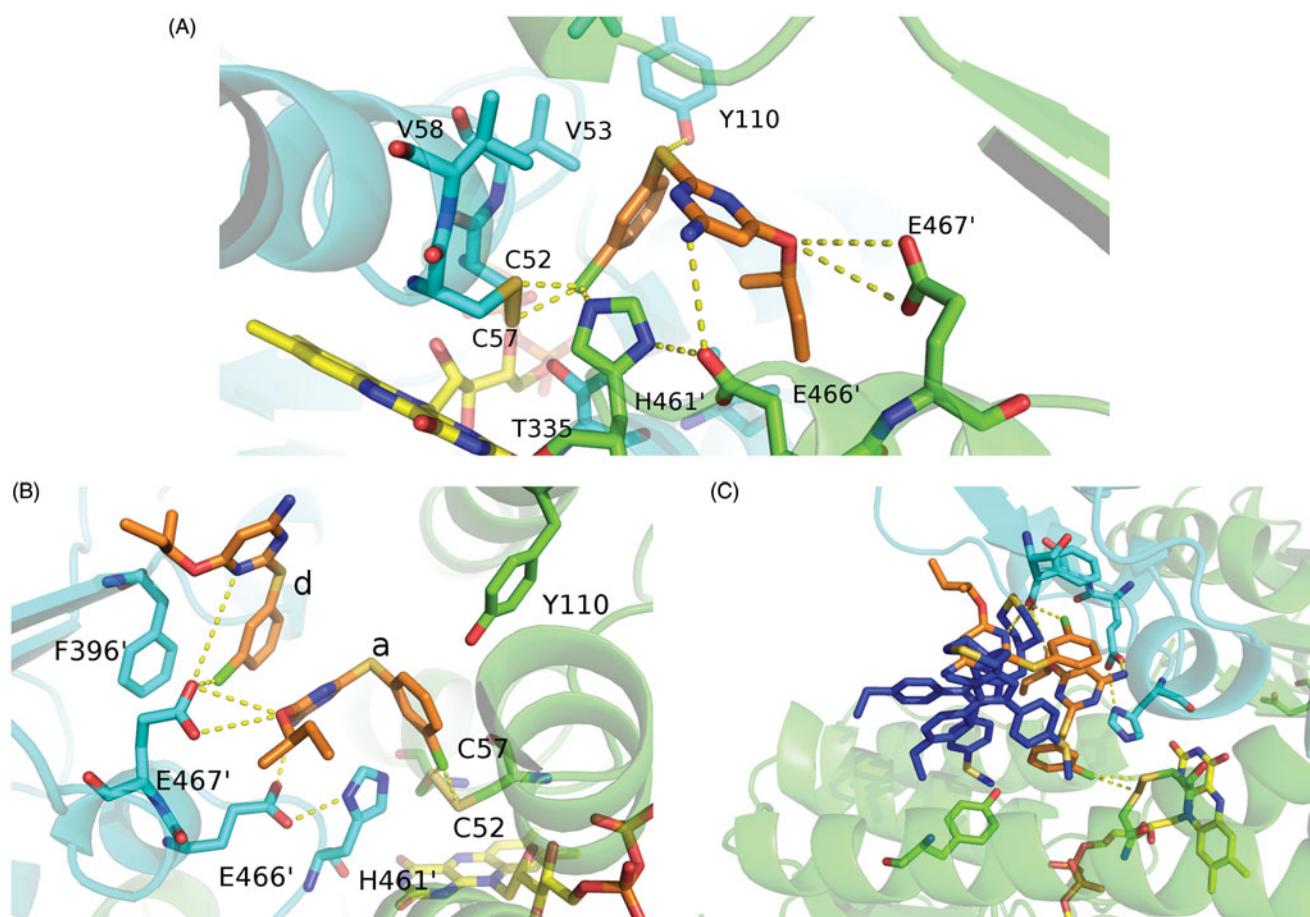


Figure 5. Blow up of the active site of TR. (A) Interaction map of RDS 777 in the TR-active site of monomer A. The residues interacting with RDS 777 are indicated and represented as sticks. (B) Interaction map of the *a* and *d* RDS777 molecules in the TR-active site of monomer B. The residues interacting with RDS 777 are indicated and represented as sticks. (C) Superimposition between the compound1-TR structure (PDB code 4APN) and RDS777-TR structure. The two molecules of compound 1 (4-((1-(4-ethylphenyl)-2-methyl-5-(4-(methylthio) phenyl)-1H-pyrrol-3 yl)methyl)thiomorpholine), RDS 777 and FAD are represented as sticks.

one of the most promising derivative in whole-cell screening assay, showing IC_{50} value in the micromolar range. Furthermore, it demonstrates high affinity for trypanothione reductase of *L. infantum*, confirming its mechanism of action as inhibitor of the aforementioned enzyme involved in the protozoan defense from oxidative damage. The X-ray structure of LiTR in complex with RDS 777 has been solved, enlightening the binding mode of our diarylsulfide derivative in the catalytic site of the protozoan enzyme. This structure shows that RDS 777 binds to the residues more involved in the catalysis, thereby impairing the catalytic activity of TR.

Nevertheless, inhibiting homolog trypanothione reductase enzymes, RDS 777 could display interesting activities also against other protozoans belonging to the Trypanosomatidae family and, thus, it could represent an useful tool for the treatment of other related neglected diseases, such as Chagas' disease (caused by *T. cruzi*) and African sleeping sickness (caused by *T. brucei*), for which, nowadays, no effective and safe therapy is available.

These data provide important insight that could be very helpful for future development of a novel class of anti-protozoan inhibitors endowed with focused structural modifications in order to increase affinity and potency against protozoan target.

Acknowledgements

We gratefully acknowledge the Helmholtz-Zentrum Berlin – Electron storage ring BESSY II for providing synchrotron radiation

at beamline BL14-1. from the European Community's Seventh Framework Program (FP7/2007–2013) under BioStruct-X (grant agreement no. 283570) and Bag Project 1223, CNCCS CNR (National Collection of Chemical Compounds and Screening Center 2015) to AI.

Disclosure statement

The authors report no conflicts of interest. The authors alone are responsible for the content and writing of this article.

Funding

CNCCS CNR (National Collection of Chemical Compounds and Screening Center 2015) [B56G15001140005].

ORCID

Luigi Scipione <http://orcid.org/0000-0002-2006-7005>
 Roberto Di Santo <http://orcid.org/0000-0002-4279-7666>
 Roberta Costi <http://orcid.org/0000-0002-1314-9029>
 Andrea Ilari <http://orcid.org/0000-0002-7754-399X>

References

- Desjeux P. Leishmaniasis: current situation and new perspectives. *Comp Immunol Microbiol Infect Dis* 2004;27:305–18.

2. Hotez PJ, Savioli L, Fenwick A. Neglected tropical diseases of the Middle East and North Africa: review of their prevalence, distribution, and opportunities for control. *PLoS Neglected Trop Dis* [Online] 2012;6:e1475. Available from: <http://journals.plos.org/plosntds/article?id=10.1371/journal.pntd.0001475>.
3. Colotti G, Baiocco P, Fiorillo A, et al. Structural insights into the enzymes of the trypanothione pathway: targets for anti-leishmaniasis drugs. *Future Med Chem* 2013;5:1861–75.
4. Fiorillo A, Colotti G, Boffi A, et al. The crystal structures of the trypanothione-trypanothione peroxidase couple unveil the structural determinants of *Leishmania* detoxification pathway. *PLoS Negl Trop Dis* [Online] 2012;6:e1781. Available from: <http://journals.plos.org/plosntds/article?id=10.1371%2Fjournal.pntd.0001781>.
5. Dumas C, Ouellette M, Tovar J, et al. Disruption of the trypanothione reductase gene of *Leishmania* decreases its ability to survive oxidative stress in macrophages. *EMBO J* 1997;16:2590–8.
6. Baiocco P, Colotti G, Franceschini S, Ilari A. Molecular basis of antimony treatment in leishmaniasis. *J Med Chem* 2009;52:2603–12.
7. Ilari A, Baiocco P, Messori L, et al. A gold-containing drug against parasitic polyamine metabolism: the X-ray structure of trypanothione reductase from *Leishmania infantum* in complex with auranofin reveals a dual mechanism of enzyme inhibition. *Amino Acids* 2012;42:803–11.
8. Baiocco P, Ilari A, Ceci P, et al. Inhibitory effect of silver nanoparticles on trypanothione reductase activity and *Leishmania infantum* proliferation. *ACS Med Chem Lett* 2010;2:230–3.
9. Ilari A, Fiorillo A, Baiocco P, et al. Targeting polyamine metabolism for finding new drugs against leishmaniasis: a review. *Mini Rev Med Chem* 2015;15:243–52.
10. Spinks D, Torrie LS, Thompson S, et al. Design, synthesis and biological evaluation of *Trypanosoma brucei* trypanothione synthetase inhibitors. *ChemMedChem* 2012;7:95–106.
11. Spinks D, Shanks EJ, Cleghorn LA, et al. Investigation of trypanothione reductase as a drug target in *Trypanosoma brucei*. *ChemMedChem* 2009;4:2060–9.
12. Massa S, Di Santo R, Costi R, et al. Synthesis of novel HEPT analogues with anti-HIV-1 activity. *Med Chem Res* 1994;4:554–62.
13. Costi R, Di Santo R, Artico M, et al. Structure-activity relationship studies on potential non-nucleoside DABO-like inhibitors of HIV-1 reverse transcriptase. *Antivir Chem Chemother* 2000;11:117–33.
14. Okauchi T, Kuramoto K, Kitamura M. Facile preparation of aryl sulfides using palladium catalysis under mild conditions. *Synlett* 2010;2891–4.
15. Sereno D, Lemesre JL. Use of an enzymatic micromethod to quantify amastigote stage of *Leishmania amazonensis* *in vitro*. *Parasitol Res* 1997;83:401–3.
16. Baiocco P, Franceschini S, Ilari A, Colotti G. Trypanothione reductase from *Leishmania infantum*: cloning, expression, purification, crystallization and preliminary X-ray data analysis. *Protein Pept Lett* 2009;16:196–200.
17. Mueller U, Darowski N, Fuchs MR, et al. Facilities for macromolecular crystallography at the Helmholtz-Zentrum Berlin. *J Synchrotron Radiat* 2012;19:442–9.
18. Kabsch W. XDS. *Acta Crystallogr D Biol Crystallogr* 2010;66:125–32.
19. Vagin AA, Teplyakov A. Molecular replacement with MOLREP. *Acta Crystallogr D Biol Crystallogr* 2010;66:22–5.
20. Murshudov GN, Vagin AA, Dodson EJ. Refinement of macromolecular structures by the maximum-likelihood method. *Acta Crystallogr D Biol Crystallogr* 1997;53:240–55.
21. Emsley P, Cowtan K. Coot: model-building tools for molecular graphics. *Acta Crystallogr D Biol Crystallogr* 2004;60:2126–32.
22. Stump B, Eberle C, Kaiser M, et al. Diaryl sulfide-based inhibitors of trypanothione reductase: inhibition potency, revised binding mode and antiprotozoal activities. *Org Biomol Chem* 2008;6:3935–47.
23. Baiocco P, Poce G, Alfonso S, et al. Inhibition of *Leishmania infantum* Trypanothione Reductase by Azole-Based Compounds: a Comparative Analysis with Its Physiological Substrate by X-ray Crystallography. *ChemMedChem* 2013;8:1175–83.
24. Krieger S, Schwarz W, Ariyanayagam MR, et al. Trypanosomes lacking trypanothione reductase are avirulent and show increased sensitivity to oxidative stress. *Mol. Microbiol* 2000;35:542–52.